Journal of the Physical Society of Japan
Vol. 66, No. 2, February, 1997, pp. 388-391

High-Order Harmonic Generation in Dense Plasmas with a High Intensity Light Field

Susumu KATO, Akio NISHIGUCHI[1], Seiji MIYAMOTO and Kunioki MIMA

Institute of Laser Engineering, Osaka University, Suita, Osaka 565
[1] *Osaka Institute of Technology, Asahi-ku, Osaka 535*

(Received July 5, 1996)

High-order harmonic generation by an oscillating current due to intense laser electric fields in dense plasmas is investigated. In solid target plasmas produced by an intense ultra-short pulse laser, the intense laser radiation directly interacts with overdense plasmas. In such a case, plasma screening effects are important in the plasma response to the laser field. For such plasmas, the higher harmonics are evaluated by using a dynamical form factor for plasma electrons and ions. There is a peak in the harmonic spectrum at twice the plasma frequency.

KEYWORDS: laser-plasma interaction, intense laser, solid target, strongly coupled plasmas, harmonic generation

Recently, nonlinear dynamics in an intense laser field has become an interesting problem. In particular, plasmas produced by ultra-short pulse lasers have attracted much interest as novel sources of radiation. The emission includes coherent radiation at harmonics of the laser frequency, discrete x-ray emission related to the bound-bound transition,[1)] and hard x-ray bremsstrahlung radiation due to high energy electrons.[2,3)] Higher harmonic generation due to the anharmonic motion of bound electrons,[4-7)] and the nonlinear response of underdense plasmas,[8-10)] overdense plasmas,[11-13)] and solids[14)] have been recently investigated theoretically. Generation of both odd and even harmonics has been observed in the interaction of an intense laser with a solid target.[15-17)]

An ultra-short pulse laser can heat a solid surface before the surface plasma expands. In such a case, the plasma density scale length is less than the laser skin depth. Consequently, the ultra-short pulse laser directly interacts with the solid-density plasma. Large space charge fluctuations are induced generating strong electrostatic waves.[18)] As a result, strongly anharmonic motion of the electrons develops, and generates higher harmonics. So far, the effects of plasma screening on high-order harmonic generation in dense plasmas have not been investigated, although the effects have been discussed for inverse bremsstrahlung absorption[19-21)] and induced electrostatic fields.[18)] Therefore, this paper investigates high-order harmonic generation involving the oscillation current which is related to the plasma polarization.

The electron density fluctuations and the vector potential are derived by using linear response theory. Ion-ion correlations and electron screening which are also included are in particular important in strongly coupled plasmas. Ion-ion coupling is usually not weak, namely $\Gamma_i \geq 1$, where Γ_i is the Coulomb coupling constant and is defined by $\Gamma_i = (Z^* e)^2/(a_i T_i)$, where $Z^* e$ is the effective ion charge, a_i is the average ion radius $(3/4\pi n_i)^{1/3}$, and T_i and n_i are the ion temperature and ion number density, respectively. For example, in the case of fully ionized solid aluminum, the Coulomb coupling constant is greater than unity, even if the ion temperature is 1.5 keV. For medium ion correlation, $1 \leq \Gamma_i \leq 10$, the ion structure factor is known to be well approximated by the hypernetted-chain equation model. The detailed formulae of the electron dielectric response function and the ion static form factor were described in previous papers.[18,19)]

Electromagnetic radiation due to current-density fluctuations in a dense plasma irradiated by an intense laser field are evaluated. We assume that the laser light is linearly polarized and the laser intensity is constant, namely $\boldsymbol{E}_L(t) = \boldsymbol{E}_0 \sin(\omega_0 t)$, where $\boldsymbol{E}_0$ and ω_0 are the laser electric field and the laser frequency, respectively. When the electron quiver speed is comparable to the speed of light, relativistic effects are important in the dynamics of the plasma. The electron motion in the perpendicular excursion length with the laser electric field is neglected in this model. Namely, only the mass correction for the electron excursion length is included. Relativistic effects are discussed in detail in the summary. The formulation is analogous to our previous paper for the induced electrostatic fields.[18)] In the following analysis, the effects of bound electrons are neglected, because the number of free electrons contributing to generating the electron density fluctuation is much greater than the number of bound electrons in highly ionized plasmas.

The electron density fluctuation in the frame that oscillates with an electron excursion length $\boldsymbol{r}_0(t)$ is obtained as:[18)]

$$\delta n_e^{osc}(\boldsymbol{r},t) = \sum_{n=-\infty}^{\infty} \exp(in\omega_0 t) \times \int \frac{d\boldsymbol{k}}{(2\pi)^3} Z^* \left[\frac{1-\epsilon(\boldsymbol{k},\omega)}{\epsilon(\boldsymbol{k},\omega)} S(\boldsymbol{k})\right] J_n(\boldsymbol{k}\cdot\boldsymbol{r}_0) \times \exp(i\boldsymbol{k}\cdot\boldsymbol{r}), \quad (1)$$

where Z^*, $S(\boldsymbol{k})$, and $\epsilon(\boldsymbol{k},\omega)$ are the charge state, the ion

form factor, and the dielectric response function, respectively, and $J_n(x)$ is a Bessel function of the first kind. The electron excursion length is $r_0 = eE_0/m_e\omega_0^2[1 + (eE_0/m_e\omega_0 c)^2/2]^{-1/2}$, where m_e, e, and c are the electron mass, the electron charge and the speed of light, respectively. This oscillating frame was introduced in the analysis of inverse bremsstrahlung in a plasma.[19,20] The electron density fluctuation in the laboratory frame is obtained as

$$\delta n_e^{lab}(\boldsymbol{r},t) = \delta n_e^{osc}(\boldsymbol{r} - \boldsymbol{r}_0(t), t). \tag{2}$$

Substituting eq. (1) into eq. (2), we have

$$\delta n_e^{lab}(\boldsymbol{r},t) = \sum_{n=-\infty}^{\infty} \exp(in\omega_0 t) \times \int \frac{d\boldsymbol{k}}{(2\pi)^3} Z^* \delta n_e^n(\boldsymbol{k}) \exp(i\boldsymbol{k}\cdot\boldsymbol{r}), \tag{3}$$

where

$$\delta n_e^n(\boldsymbol{k}) = \sum_{n=-\infty}^{\infty} F^m(\boldsymbol{k}) B_n^m(\boldsymbol{k}\cdot\boldsymbol{r}_0), \tag{4}$$

$$F^m(\boldsymbol{k}) = Z^* \left[\frac{1-\epsilon(\boldsymbol{k},\omega)}{\epsilon(\boldsymbol{k},\omega)} S(\boldsymbol{k})\right], \tag{5}$$

$$B_n^m(\boldsymbol{k}\cdot\boldsymbol{r}_0) = J_m(\boldsymbol{k}\cdot\boldsymbol{r}_0) J_{m-n}(\boldsymbol{k}\cdot\boldsymbol{r}_0). \tag{6}$$

$F^m(x)$ and $B_n^m(x)$ represent the plasma screening function and nonlinearity associated with the finite electron excursion length, respectively.

The current density induced in the plasma through coupling between the laser and the density fluctuations is obtained as discussed in ref. 22. The Fourier components of the current-density fluctuations are

$$\boldsymbol{J}(\boldsymbol{k},\omega) = \frac{e^2 n_e \boldsymbol{E}_0}{2m_e\omega}[\delta n_e(\boldsymbol{r},\omega-\omega_0) - \delta n_e(\boldsymbol{r},\omega+\omega_0)], \tag{7}$$

where n_e is the electron density and $\delta n_e(\boldsymbol{k},\omega)$ are the Fourier components of the electron density fluctuation given by eq. (3):

$$\delta n_e(\boldsymbol{k},\omega) = \sum_{n=-\infty}^{\infty} F^m(\boldsymbol{k}) B_n^m(\boldsymbol{k}\cdot\boldsymbol{r}_0) 2\pi\delta(\omega - n\omega_0). \tag{8}$$

The Fourier components of the vector potential $\boldsymbol{A}_\omega(\boldsymbol{r})$ far away from the emission region are determined as follows:

$$\boldsymbol{A}_\omega(\boldsymbol{r}) = \frac{\exp(i\boldsymbol{k}_{em}\cdot\boldsymbol{r})}{cr} \times \int_V \boldsymbol{J}_\omega(\boldsymbol{r}')\exp(-i\boldsymbol{k}_{em}\cdot\boldsymbol{r}')d\boldsymbol{r}', \tag{9}$$

where $\boldsymbol{k}_{em}$, and V are the wave number and the volume of plasma, respectively, and $\boldsymbol{J}_\omega(\boldsymbol{r})$ is the temporal Fourier component of the current. Substituting eq. (7) into eq. (9), we obtain the vector potential as follows:

$$\boldsymbol{A}_{N\omega_0}(\boldsymbol{r}) = \frac{e^2 n_e V \boldsymbol{E}_0}{2m_e N\omega_0} \times \frac{\exp(i\boldsymbol{k}_{em}^N\cdot\boldsymbol{r})}{cr}\alpha(\boldsymbol{k}_{em}^N, N\omega_0), \tag{10}$$

where

$$\alpha(\boldsymbol{k}, N\omega_0) = \sum_{n=-\infty}^{\infty} F^m(\boldsymbol{k}) J_m(\boldsymbol{k}\cdot\boldsymbol{r}_0) \times [J_{m+N-1}(\boldsymbol{k}\cdot\boldsymbol{r}_0) - J_{m+N+1}(\boldsymbol{k}\cdot\boldsymbol{r}_0)]. \tag{11}$$

Here $\boldsymbol{k}_{em}^N$ is the wave number of the N-th order harmonic emission.

The spectral radiation power per unit solid angle is obtained from eq. (10) as follows,

$$\frac{dP_{N\omega_0}}{d\Omega} = \frac{1}{4}\frac{cE_0^2}{8\pi}\left[\frac{\boldsymbol{k}_{em}^N c}{N\omega_0}\right]^2 \times r_e^2 \left|\alpha(\boldsymbol{k}_{em}^N, N\omega_0)\right|^2 \sin^2\theta (n_e V)^2, \tag{12}$$

where $r_e = e^2/m_e c^2$ is the classical electron radius and θ is the angle between $\boldsymbol{E}_0$ and $\boldsymbol{k}_{em}^N$.

Electrons do not instantaneously respond to the laser field. Therefore, dynamic screening effects are essential

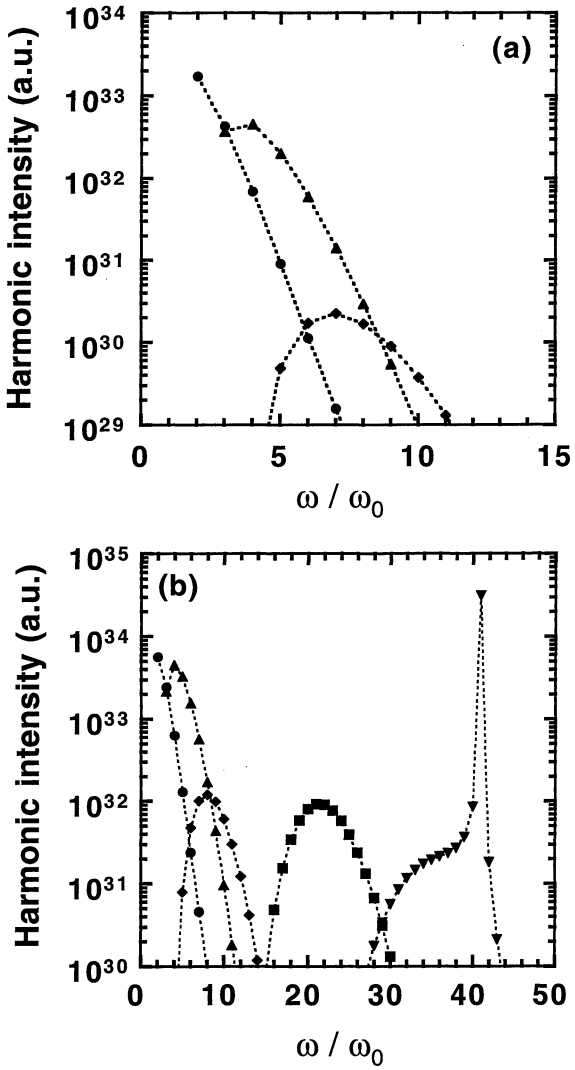

Fig. 1. Total power spectrum of electromagnetic radiation as a function of the laser intensity. The circle, triangle, diamond, square, and inverse triangle show $n_e = n_c$, $4n_c$, $10n_c$, $100n_c$, and n_s, respectively. (a) and (b) are for $I_L = 1 \times 10^{18}$ W/cm^2 and 2×10^{18} W/cm^2, respectively.

for high-order harmonic generation. If the dielectric electron response function does not depend on the frequency, namely $F^m(x) \simeq F(x)$, the time dependence of the electron density fluctuation vanishes. So, the summation of eq. (11) over m vanishes. The plasma screening factor F^m has a peak at $|m| \approx \omega_p/\omega_0 = (n_e/n_c)^{1/2}$, namely, the frequency is in resonance near the plasma frequency, when $k_{em}^N \ll k_D$.

The total power spectra for overdense plasmas are calculated by integrating eq. (12) over all solid angles. Here we assume that the laser wavelength is 0.53 μm, and the cutoff density n_c is 4.0×10^{21} cm^{-3}. The ion temperature is assumed to be same as the electron temperature which is 1 keV. For fully ionized aluminum, the solid density n_s is 8.6×10^{23} cm^{-3}, namely, $n_s/n_c = 215$. The volume V depends on the skin depth c/ω_p, where ω_p is the plasma frequency. However, we assumed that the volume is constant.

Figures 1(a) and 1(b) show the electron density dependencies of the power spectra when the laser intensities are 1×10^{18} W/cm^2 and 2×10^{18} W/cm^2, respectively. The peaks of the spectra are at $N \approx 2(n_s/n_c)^{1/2}$. The higher harmonics are localized between $16\omega_0$ and $30\omega_0$ for $n_e = 100n_c$ and between $28\omega_0$ and $43\omega_0$ for $n_e = n_s$. For $n_e = n_s$ in Fig. 1(b), there is a peak at $N = 41$, because in the vicinity of $N \approx 41$ and $m = 15$, the wave number of electromagnetic wave coincides with the wave number of the plasma wave. The imaginary part of the dielectric function is negligible. In such a case, the electron-ion collision frequency becomes important for

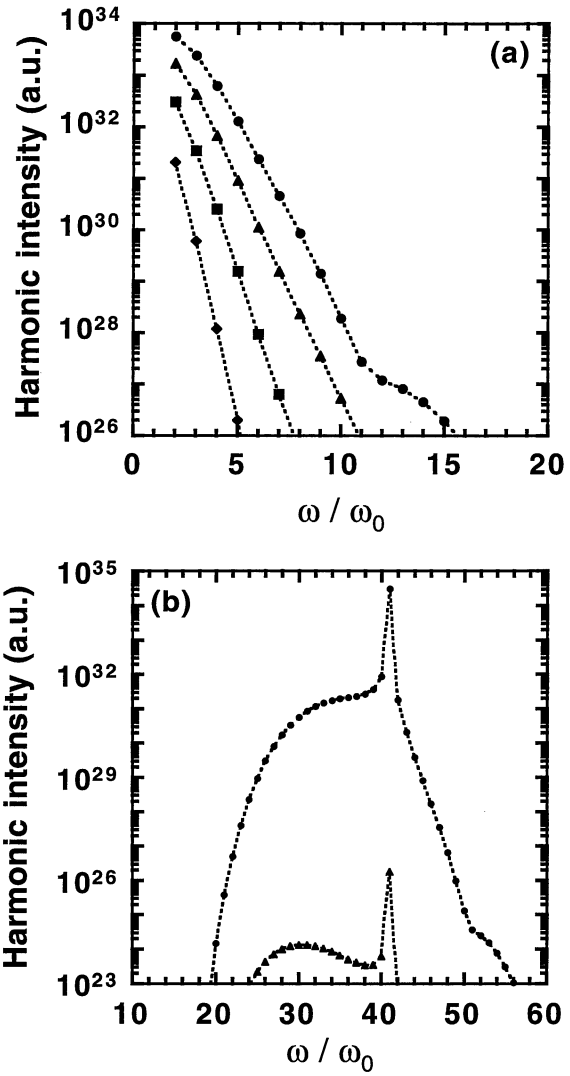

Fig. 2. Total power spectrum of electromagnetic radiation as a function of the electron density. The diamond, square, triangle, and circle show $I_L = 1 \times 10^{17}$ W/cm^2, 4×10^{17} W/cm^2, 1×10^{18} W/cm^2, and 2×10^{18} W/cm^2, respectively. (a) and (b) are for the cutoff and solid densities, respectively.

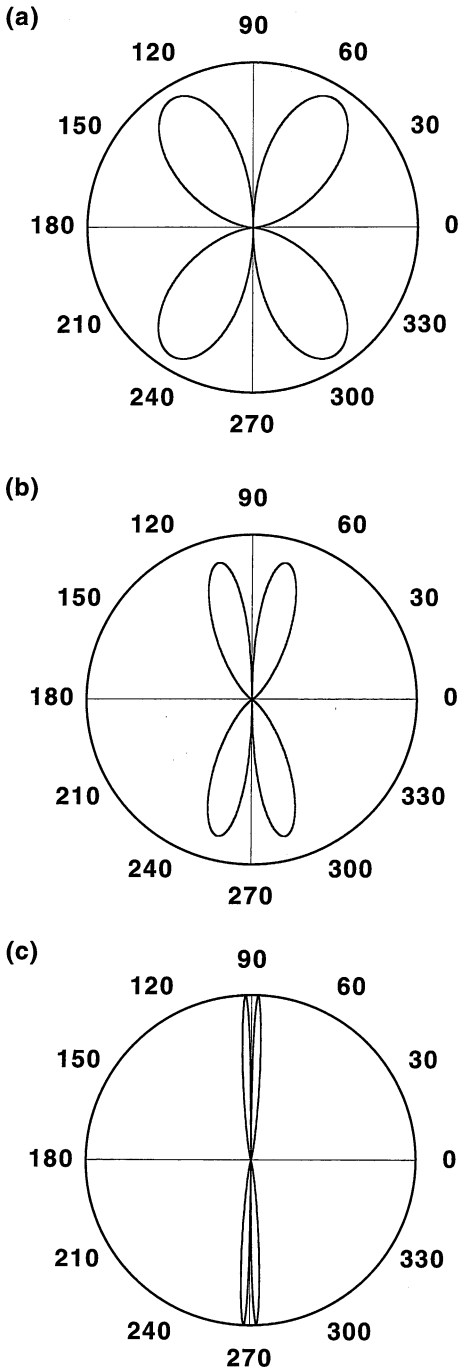

Fig. 3. The angular distribution of the high-order harmonics. The zero direction is along the electric field. (a) and (b) show the second and fifth order harmonics, respectively, for the cutoff density with $I_L = 2 \times 10^{18}$ W/cm^2. (c) shows the thirtieth order harmonic for the solid density with $I_L = 2 \times 10^{18}$ W/cm^2.

the damping of the wave. However, this model does not include collisional processes. The sharp spectral peak will be actually broadened by the collision.

Figures 2(a) and 2(b) show the laser intensity dependencies of the power spectra for the cutoff and solid densities, respectively. For the cutoff density in Fig. 2(a), the power of second and fifth order harmonics for $I_L = 1 \times 10^{18}$ W/cm^2 are 10^2 and 10^6 times greater than the harmonics for $I_L = 1 \times 10^{17}$ W/cm^2, respectively. The generation of high-order harmonics strongly depends on the laser intensity. For the solid-density plasma in Fig. 2(b), the peak power of the high-order harmonics for $I_L = 2 \times 10^{18}$ W/cm^2 is 10^8 times greater than the harmonics for $I_L = 1 \times 10^{18}$ W/cm^2.

The angular distributions of the high-order harmonics are shown in Figs. 3. For the cutoff density with $I_L = 2\times10^{18}$ W/cm^2, Figs. 3(a) and 3(b) show the second and fifth order harmonics, respectively. Figure 3(c) shows the thirtieth order harmonic for the solid density with $I_L = 2 \times 10^{18}$ W/cm^2. These patterns have the directionality. In Fig. 3(c), the propagation direction is perpendicular to the electron excursion direction, namely the laser electric field direction.

In summary, we have derived a formula for electron density fluctuations around an ion in a dense plasma irradiated by an intense laser field. The total power spectra of the electromagnetic radiation due to the electron density fluctuations are evaluated. There are both odd and even harmonics due to the nonlinear response of the electron density fluctuations. As a result, harmonics above $30\omega_0$ appear for fully ionized aluminum at the solid density interacting with a laser pulse of intensity $I_L = 2\times10^{18}$ W/cm^2. They are strongly directed in the plane perpendicular to the laser electric field [See Fig. 3(c)]. The harmonics below $10\omega_0$ are generated near the cutoff density.

Finally, we discuss the limitation of our theory. The electron quiver velocity is comparable to the speed of light, when the laser intensity $I_L\lambda^2$ is higher than 10^{18} Wμm^2/cm^2, where I_L and λ^2 are the laser intensity and wavelength, respectively. In this paper, relativistic effects are only treated by mass correction, namely, our present formula is no longer valid, when relativistic effects are essential for plasma dynamics. In the relativistic regime, highly nonlinear processes are reported from particle-in-cell code simulation.[23-25] Especially, a harmonic generation mechanism that has no cut off at the plasma frequency is reported by Gibbon.[25] This mechanism of harmonic generation is completely different from our mechanism which is induced by nonlinear dense plasma polarization in the screened ion potential.

We would like to thank Professor K. Nishihara and H. Takabe of the Institute of Laser Engineering, Osaka University and Dr. H. Furukawa of the Institute for Laser Technology for fruitful discussions. This work was partially supported by Research Aid of Inoue Foundation for Science, the Grant-in-Aid for Scientific Research from the Ministry of Education, Science and Culture of Japan and Fellowships of the Japan Society for the Promotion of Science.

1) M. Chaker, J. C. Kieffer, J. P. Matte, H. Pepin, P. Audebert, P. Maine, D. Strickland, P. Bado and G. Mourou: Phys. Fluids B **3** (1991) 167.
2) J. D. Kmetec, C. L. Gordon III, J. J. Macklin, B. E. Lemoff, G. S. Brown and S. E. Harris: Phys. Rev. Lett. **68** (1992) 1527.
3) B. N. Chichkov, Y. Kato and M. Murakami: Phys. Rev. A **46** (1992) 4512.
4) K. C. Kulander and B. W. Shore: Phys. Rev. Lett. **62** (1989) 524.
5) J. H. Eberly, Q. Su and J. Javanainan: J. Opt. Soc. Am. B **6** (1989) 1289.
6) J. L. Krause, K. J. Schafer and K. C. Kulander: Phys. Rev. Lett. **68** (1992) 3535.
7) V. C. Reed and K. Burnett: Phys. Rev. A **46** (1992) 424.
8) F. Brunel: J. Opt. Soc. Am. B **7** (1990) 521.
9) P. Sprangle, E. Esarey and A. Ting: Phys. Rev. A **41** (1990) 4463; P. Sprangle, E. Esarey and A. Ting: Phys. Rev. Lett. **64** (1990) 2011.
10) J. M. Rax and N. J. Fisch: Phys. Rev. Lett. **69** (1992) 772.
11) S. C. Wilks, W. L. Kruer and W. B. Mori: IEEE Trans. Plasma Sci. **21** (1993) 120.
12) B. Bezzerides, R. D. Jones and D. W. Forslund: Phys. Rev. Lett. **49** (1982) 202.
13) C. Grebogi, V. K. Tripithi and H. H. Chen: Phys. Fluids **26** (1983) 1904.
14) S. Hüller and J. Meyer-ter-Vhen: Phys. Rev. **48** (1993) 3906.
15) R. L. Carman, D. W. Forslund and J. M. Kindel: Phys. Rev. Lett. **46** (1981) 29.
16) Gy. Farkas, Cs. Tóth, S. D. Moustaizis, N. A. Papadogiannis and C. Fotakis: Phys. Rev. A **46** (1992) R3605.
17) D. von der Linde, T. Engers, G. Jenke, P. Agostini, G. Grillon, E. Nibbering, A. Mysyrowicz and A. Antonetti: Phys. Rev. A **52** (1995) R25.
18) S. Kato, A. Nishiguchi and K. Mima: Phys. Rev. E **50** (1994) 2193.
19) S. Kato, R. Kawakami and K. Mima: Phys. Rev. A **43** (1991) 5560.
20) J. Dawson and C. Oberman: Phys. Fluids **5** (1962) 517.
21) R. D. Jones and K. Lee: Phys. Fluids **25** (1982) 2307.
22) S. Ichimaru: *Basic Principles of Plasma Physics* (Benjamin, Massachusetts, 1973).
23) S. C. Wilks, W. L. Kruer, M. Tabak and A. B. Langdon: Phys. Rev. Lett. **69** (1992) 1383.
24) P. Gibbon: Phys. Rev. Lett. **73** (1994) 664.
25) P. Gibbon: Phys. Rev. Lett. **76** (1996) 50.